Observation of acoustic plasma waves with a velocity approaching the speed of light

I. V. Andreev,* V. M. Muravev,* N. D. Semenov, and I. V. Kukushkin
Institute of Solid State Physics, RAS, Chernogolovka, 142432 Russia

(Received 21 September 2020; revised 24 February 2021; accepted 25 February 2021; published 15 March 2021)

We investigate the electrodynamics of a disk-shaped two-dimensional electron system in the proximity of a screening gate. The two-dimensional plasmons in the system under study exhibit the linear dispersion characteristic of acoustic plasma waves. We experimentally achieve the limit when the velocity of acoustic waves approaches the speed of light. We show that retardation effects lead to strong coupling between acoustic plasmons and the light, which is manifested in the renormalization of the electron effective mass. We develop a theory to substantiate the observed phenomena.

DOI: 10.1103/PhysRevB.103.115420

I. INTRODUCTION

Acoustic waves in gaseous and solid-state media are among the most common occurrences in nature. Examples of acoustic excitations include ordinary sound waves, zero-sound vibrations in quantum Fermi liquids, and Bogolyubov waves in correlated bosonic systems. For most of them, the velocity does not exceed $V_s = c_0/300$, where $c_0 = 3 \times 10^8$ m/s is the speed of light. However, the relativistic regime, when the velocity of acoustic waves becomes comparable to the speed of light and polaritonic effects become significant, remains much less explored. Understanding the behavior of matter under such conditions is one of the most outstanding open problems in modern physics, with possible implications in the areas of ultrastrong light-matter coupling [1–3], new photonic states of matter [4–6], and even the neutron star instability against collapse into a black hole [7,8].

One of the representatives of the family of the acoustic waves is a two-dimensional (2D) plasma wave propagating in a solid-state two-dimensional electron system (2DES) placed in the vicinity of a back gate [9–18]. In this case, screening of the Coulomb interaction of charges in the 2DES leads to the following linear dispersion law of acoustic plasmons [9]:

$$\omega_{\mathrm{AP}} = \sqrt{\frac{n_s e^2 h}{\varepsilon \varepsilon_0 m^*}} q = V_p q \quad (qh \ll 1), \tag{1}$$

where ω_{AP} is the acoustic plasmon frequency, V_p is the acoustic plasmon velocity in the quasistatic approximation, q is the wave vector of the plasmon, h is the distance between the conducting gate and the 2DES, n_s and m^* are the density and effective mass of the 2D electrons, and ε_0 and ε denote the electric constant and effective permittivity of the semiconductor crystal between the back gate and 2DES, respectively. The electric field of such a wave is localized in the semiconductor substrate. For this reason, Eq. (1) contains the total dielectric permittivity of the substrate ε. In view of the above, it should be mentioned that for a number of years, the velocity of acoustic plasmons was considered to be very small due to the screening of the Coulomb interaction.

In this paper, we report on the experimental results of achieving the limit of $V_p/c > 1$ (with $c = c_0/\sqrt{\varepsilon}$ being the speed of light in the semiconductor substrate hosting the 2DES), when relativistic retardation effects start to play a significant role. We show that the retardation effects cause strong interaction of acoustic plasmons with the light, which renormalizes both plasma frequency at zero magnetic field and acoustic plasmon behavior in a magnetic field. Both of these effects can be simultaneously described through the giant renormalization of the effective mass of the charge carriers [19–21]:

$$m = m^*\left(1 + \frac{V_p^2}{c^2}\right). \tag{2}$$

II. EXPERIMENTAL TECHNIQUE

The experiments were carried out on semiconductor heterostructures with a single GaAs/$Al_xGa_{1-x}As$ ($x = 0.3$) quantum well of 20-nm width. We investigated the samples with the electron density $n_s = 7.5 \times 10^{11}$ cm^{-2} and electron mobility $\mu = 0.4 \times 10^6$ cm^2/(V s) at the temperature $T = 4.2$ K. The disk-shaped mesas of diameter $D = 4$ and 6 mm were fabricated from the quantum well on the top surface of the sample by means of optical lithography and wet chemical etching. The metallic gate was deposited on the bottom surface of the semiconductor substrate. The distance h separating the quantum well and the gate was adjusted in the range of 140–640 μm at the manufacturing stage by polishing the GaAs substrate. Plasmons in the samples were excited with the electromagnetic field from either a rectangular waveguide or a wire antenna. Plasma resonances in the 2DES were detected using a noninvasive optical technique based on the ultrahigh sensitivity of the recombination photoluminescence spectrum of 2D electrons in GaAs, even to minor heating caused by the resonant microwave absorption. The system was continuously illuminated by a laser with

*These authors contributed equally to this work.

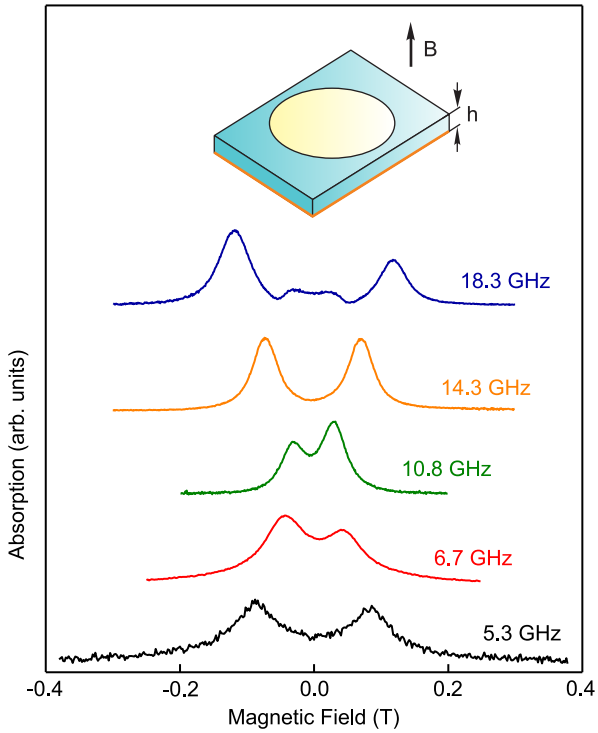

FIG. 1. Microwave absorption curves plotted as a function of the magnetic field for five excitation frequencies. The measurements are taken for the sample with 2DES diameter $D = 4$ mm, electron density $n_s = 7.5 \times 10^{11}$ cm^{-2}, and substrate thickness $h = 640$ μm. The inset depicts the sample schematic with the back gate marked in orange at the bottom surface of the substrate.

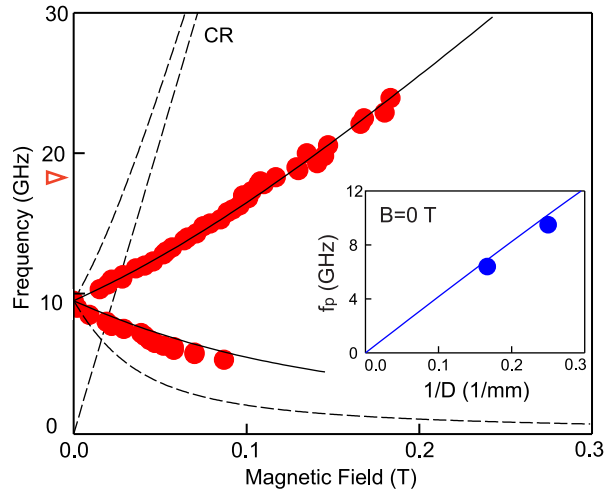

FIG. 2. Magnetodispersion of the acoustic 2D plasmon observed in the sample with 2DES disk diameter $D = 4$ mm, electron density $n_s = 7.5 \times 10^{11}$ cm^{-2}, and substrate thickness $h = 640$ μm (red dots). Dashed curves represent the low- and high-frequency branches, ω_- and ω_+, respectively. The dashed straight line indicates the cyclotron resonance (CR) magnetodispersion $\omega = eB/m^*$. Solid lines represent fits of the experimental points according to Eq. (3) with renormalized effective electron mass. The red arrowhead marks the calculated nonretarded plasmon frequency $f_{AP} = 18.2$ GHz. The inset shows the dispersion of the acoustic 2D plasmon at zero magnetic field, with the solid line denoting the theoretical prediction calculated from Eq. (4). The plasmon velocity is $v = \omega/q = 0.8c$.

780-nm wavelength, which created a quasistationary population of photoexcited holes in the GaAs quantum well. The 2D electrons recombinate radiatively with these photoexcited 2D holes, and the recombination luminescence spectrum turns out to be extremely sensitive to the temperature of the 2DES. Recombination spectra with and without microwave excitation of the 2DES were recorded and analyzed with a spectrometer and a CCD camera. The integral of the absolute value of the difference of these two spectra is a quantitative measure of the system heating, i.e., the microwave absorption. This technique is described in detail elsewhere [22,23]. All measurements were taken in a liquid helium cryostat with a superconducting coil at $T = 4.2$ K. The magnetic field of 0–0.4 T was directed perpendicular to the sample surface.

III. RESULTS AND DISCUSSION

Figure 1 shows typical microwave absorption curves as a function of the magnetic field, obtained for the sample with electron density $n_s = 7.5 \times 10^{11}$ cm^{-2} and GaAs substrate thickness $h = 640$ μm. All data plots demonstrate a pronounced microwave absorption resonance, symmetric with respect to the zero magnetic field. To further examine the nature of the resonance, we include its magnetodispersion in Fig. 2, marked with the red dots. Here, the low-frequency branch (ω_-) corresponds to the excitation of the edge magnetoplasmon (EMP). In a qualitative sense, this mode originates from the skipping-orbit collective motion of electrons along the edge of the 2DES. The high-frequency branch (ω_+) in Fig. 2 refers to the excitation of the cyclotron magnetoplasma mode arising from the collective motion of electrons in cyclotron orbits throughout the entire area of the 2DES. It should be noted that the observed behavior is similar to that of acoustic plasma waves measured in 2DES disks when retardation effects are small [24]. Magnetodispersion in Fig. 2 is accurately described using dipole approximation [25]:

$$\omega_\pm = \pm\frac{\omega_c}{2} + \sqrt{\left(\frac{\omega_c}{2}\right)^2 + \omega_p^2}, \tag{3}$$

where ω_p is the experimentally determined plasma frequency at zero magnetic field and $\omega_c = eB/m$ is the effective cyclotron frequency.

Importantly, the resonant plasma frequency at zero magnetic field is appreciably lower than the nonretarded value $f_{AP} = 18.2$ GHz (marked by the red arrowhead in Fig. 2) calculated from Eq. (1) for $m^* = 0.067m_0$, the dielectric permittivity $\varepsilon = 12.8$, and the wave vector $q \approx 3.7/D$ [26]. Another crucial observation in Fig. 2 is that the upper cyclotron magnetoplasma mode intersects the cyclotron resonance line $\omega_c = eB/m^*$ (straight dashed line) instead of tending to it asymptotically (as shown by the dashed curve). Both phenomena make it evident that relativistic retardation effects substantially modify the spectrum of acoustic plasmons, which is consistent with the fact that the quasistatic plasmon velocity $V_p = \omega_{AP}/q = 1.5c$.

To quantitatively account for the retardation effects in the spectrum of acoustic 2D plasmons, we adapt the theoretical concepts from the case of an infinite 2DES [19–21] to the

bounded disk geometry. The details of the developed theory are provided in the Supplemental Material [27]. According to our prediction, retardation effects result in simultaneous renormalization of plasma and cyclotron frequencies

$$\omega_p = \frac{\omega_{\rm AP}}{\sqrt{1+\dfrac{V_p^2}{c^2}}}, \tag{4}$$

$$\omega_c = \frac{eB/m^*}{1+\dfrac{V_p^2}{c^2}}. \tag{5}$$

Notably, both of these effects can be accounted for by renormalization of a single quantity—the effective electron mass $m = m^*(1+V_p^2/c^2)$.

To further test our hypothesis, we compare the experimental data with the developed theory. For the given sample, we find the experimentally obtained plasma frequency $f_p = 9.5$ GHz to be approximately twice as low as the nonretarded value $f_{\rm AP} = 18.2$ GHz. At the same time, the experimentally determined renormalization factor $f_{\rm AP}/f_p = 1.9$ is in good agreement with the theoretical estimate of $\sqrt{1+V_p^2/c^2} = 1.8$, where $V_p = \omega_{\rm AP}/q = 1.5c$. Another way to compare the experiment with the theory is to analyze the magnetic field behavior of the acoustic plasma wave. The best fit of Eq. (3) to the magnetodispersion data in Fig. 2 yields $eB/m^*\omega_c = 3.6$, which likewise agrees reasonably well with the theoretical prediction of $1+V_p^2/c^2 = 3.3$. Interestingly, retardation does not affect the linear dispersion characteristic of acoustic waves. Indeed, as shown in the inset of Fig. 2, the measurement results for the disk diameters $D = 4$ and 6 mm (blue dots) closely follow the linear dispersion (solid line) calculated from Eqs. (1) and (4), which further proves the given plasma mode to be an acoustic wave. From the inset we can directly determine the actual velocity of the plasma wave $v = \omega_p/q = 0.8c$, which is very close to the speed of light in the substrate c.

One of the most compelling features of acoustic plasma waves in the relativistic regime is the tunability of the effective electron mass through the variation of either the electron density n_s or the distance h between the 2DES and the conducting gate. In fact, according to Eqs. (2) and (4), the effective electron mass can be expressed as

$$\frac{m}{m^*} = \left(\frac{f_{\rm AP}}{f_p}\right)^2 = 1+\frac{V_p^2}{c^2} = 1+\frac{n_s e^2 h}{\varepsilon_0 m^* c_0^2}. \tag{6}$$

Therefore m/m^* is expected to be linearly dependent on the substrate thickness h. To compare this prediction against the measurement data, Fig. 3 includes the experimental results for m/m^*, obtained for $h = 640, 475, 380, 340, 280, 215,$ and 140 μm, where all seven samples have fixed 2DES mesa diameter $D = 4$ mm and electron density $n_s = 7.5\times 10^{11}$ cm^{-2}. Clearly, all the experimental data points exhibit nearly perfect linear behavior following a straight line with a slope of 4.2 mm^{-1}, which closely agrees with the theoretical value of $n_s e^2/\varepsilon_0 m^* c_0^2 = 4.0$ mm^{-1}. We start from $m/m^* = (3.7\pm 0.1)$ for the sample, where hybridization with light plays the most significant role, and end at the point $m/m^* = 1$ for the linear extrapolation of the experimental data in Fig. 2 to $h = 0$. This behavior is in agreement with the prediction of Eq. (6). Such a degree of consistency between the analytical and experimental results confirms the validity of the developed theory. Thus we have experimentally verified that the spacing between the 2DES and back gate controls the interaction between 2D plasma and light.

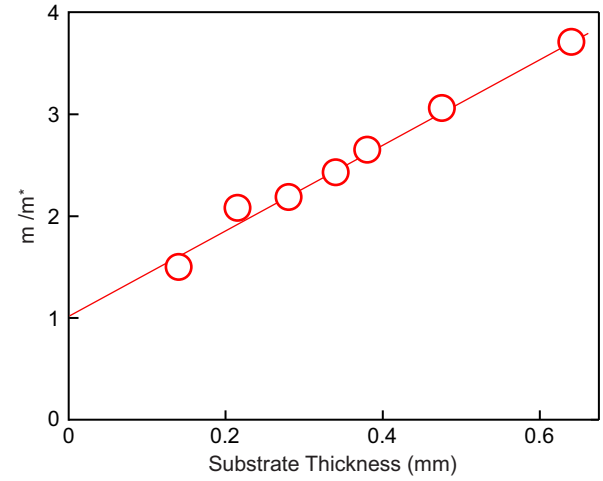

FIG. 3. Dependence of the normalized electron mass m/m^* on the substrate thickness h. Experimental data correspond to the 2DES with fixed disk geometry, $D = 4$ mm, and electron density $n_s = 7.5\times 10^{11}$ cm^{-2}. The solid line is a linear fit to the experimental data.

IV. SUMMARY AND CONCLUSIONS

In conclusion, we have explored acoustic plasma waves in a 2DES screened with a metallic gate on the substrate back side. Due to carefully selected structure parameters, we were able to reach the limit where the acoustic wave velocity approaches the speed of light in the semiconductor substrate, $v = 0.8c$, when acoustic plasmons interact strongly with light. The strength of the light-plasmon interaction could be controlled by varying substrate thickness or electron density. We find that retardation effects lead to significant changes in the plasma wave velocity and magnetic field behavior. We show that both phenomena can be accounted for by the renormalization of the electron effective mass, $m = m^*(1+V_p^2/c^2)$. The studied regime of the acoustic wave propagation is interesting since it not only may be relevant to the physics of 2D electron structures but also, for instance, can be a precursor of a transition to the new photonic states of matter and have relevance to the physics of black hole formation.

ACKNOWLEDGMENTS

We thank V. A. Volkov and A. A. Zabolotnykh for their advice in the derivation of Eqs. (4) and (5). The authors gratefully acknowledge the financial support of the Russian Science Foundation (Grant No. 19-72-30003).

[1] V. M. Muravev, I. V. Andreev, I. V. Kukushkin, S. Schmult, and W. Dietsche, Phys. Rev. B **83**, 075309 (2011).
[2] G. Scalari, C. Maissen, D. Turcinkova, D. Hagenmüller, S. De Liberato, C. Ciuti, C. Reichl, D. Schuh, W. Wegscheider, M. Beck, and J. Faist, Science **335**, 1323 (2012).
[3] Q. Zhang, M. Lou, X. Li, J. L. Reno, W. Pan, J. D. Watson, M. J. Manfra, and J. Kono, Nat. Phys. **12**, 1005 (2016).
[4] Y. K. Wang and F. T. Hioe, Phys. Rev. A **7**, 831 (1973).
[5] G. Mazza and A. Georges, Phys. Rev. Lett. **122**, 017401 (2019).
[6] F. Schlawin, A. Cavalleri, and D. Jaksch, Phys. Rev. Lett. **122**, 133602 (2019).
[7] S. A. Bludman and M. A. Ruderman, Phys. Rev. **170**, 1176 (1968).
[8] M. Ruderman, Phys. Rev. **172**, 1286 (1968).
[9] A. V. Chaplik, Zh. Eksp. Teor. Fiz. **62**, 746 (1972) [Sov. Phys. JETP **35**, 395 (1972)].
[10] U. Mackens, D. Heitmann, L. Prager, J. P. Kotthaus, and W. Beinvogl, Phys. Rev. Lett. **53**, 1485 (1984).
[11] P. J. Burke, I. B. Spielman, J. P. Eisenstein, L. N. Pfeiffer, and K. W. West, Appl. Phys. Lett. **76**, 745 (2000).
[12] V. M. Muravev, C. Jiang, I. V. Kukushkin, J. H. Smet, V. Umansky, and K. von Klitzing, Phys. Rev. B **75**, 193307 (2007).
[13] W. F. Andress, H. Yoon, K. Y. M. Yeung, L. Qin, K. West, L. Pfeiffer, and D. Ham, Nano Lett. **12**, 2272 (2012).
[14] J. Chen, M. Badioli, P. Alonso-Gonzalez, S. Thongrattanasiri, F. Huth, J. Osmond, M. Spasenovic, A. Centeno, A. Pesquera, P. Godignon, A. Zurutuza Elorza, N. Camara, F. Abajo, R. Hillenbrand, and F. H. L. Koppens, Nature (London) **487**, 77 (2012).
[15] Z. Fei, A. S. Rodin, G. O. Andreev, W. Bao, A. S. McLeod, M. Wagner, L. M. Zhang, Z. Zhao, M. Thiemens, G. Dominguez, M. M. Fogler, A. H. Castro Neto, C. N. Lau, F. Keilmann, and D. N. Basov, Nature (London) **487**, 82 (2012).
[16] G. C. Dyer, G. R. Aizin, S. J. Allen, A. D. Grine, D. Bethke, J. L. Reno, and E. A. Shaner, Nat. Photonics **7**, 925 (2013).
[17] D. A. Iranzo, S. Nanot, E. J. C. Dias, I. Epstein, C. Peng, D. K. Efetov, M. B. Lundeberg, R. Parret, J. Osmond, J.-Y. Hong, J. Kong, D. R. Englund, N. M. R. Peres, and F. H. L. Koppens, Science **360**, 291 (2018).
[18] D. A. Bandurin, D. Svintsov, I. Gayduchenko, S. G. Xu, A. Principi, M. Moskotin, I. Tretyakov, D. Yagodkin, S. Zhukov, T. Taniguchi, K. Watanabe, I. V. Grigorieva, M. Polini, G. N. Goltsman, A. K. Geim, and G. Fedorov, Nat. Commun. **9**, 5392 (2018).
[19] Yu. A. Kosevich, A. M. Kosevich, and J. C. Granada, Phys. Lett. A **127**, 52 (1988).
[20] A. V. Chaplik, Pis'ma Zh. Eksp. Teor. Fiz. **101**, 602 (2015) [JETP Lett. **101**, 545 (2015)].
[21] A. A. Zabolotnykh and V. A. Volkov, Phys. Rev. B **103**, 125301 (2021).
[22] I. V. Kukushkin, J. H. Smet, K. von Klitzing, and W. Wegscheider, Nature (London) **415**, 409 (2002).
[23] V. M. Muravev, I. V. Andreev, S. I. Gubarev, V. N. Belyanin, and I. V. Kukushkin, Phys. Rev. B **93**, 041110(R) (2016).
[24] S. I. Gubarev, V. M. Muravev, I. V. Andreev, V. N. Belyanin, and I. V. Kukushkin, Pis'ma Zh. Eksp. Teor. Fiz. **102**, 517 (2015) [JETP Lett. **102**, 461 (2015)].
[25] S. J. Allen, Jr., H. L. Störmer, and J. C. M. Hwang, Phys. Rev. B **28**, 4875(R) (1983).
[26] A. L. Fetter, Phys. Rev. B **33**, 5221 (1986).
[27] See Supplemental Material at http://link.aps.org/supplemental/10.1103/PhysRevB.103.115420 for the theoretical treatment of retardation effects in the spectrum of 2D plasmons with strong screening in a disk-shaped geometry.